MSB1007 Integration Assignment:

Cardiac Electrophysiology Simulation

Student name: Mai Le
ID: i6375777

Introduction

Brugada syndrome (BrS) is a genetic cardiac disorder characterized by the right bundle branch block and ST-segment elevation in the right precordial leads (V1-V3) in the ECG image (1). This disorder can lead to high potential life-threatening arrhythmias like ventricular tachycardia or fibrillation (2). If these arrhythmias are sustained, they may result in an increased risk of sudden cardiac deaths (up to 20%) in patients with structurally normal hearts (2). The most common mutation in BrS is found in the *SCN5A* gene of approximately 15 – 30% of patients (1). *SCN5A* encodes for pore-forming α-subunit of Nav1.5 channels which are responsible for triggering the action potential (AP) and driving electric impulse transmission of myocytes (3). *SCN5A* mutation leads to reduced Na+ current which is associated with slow or blocked conduction and heterogeneous repolarization, creating a potentially proarrhythmic substrate (4). Despite these insights, the link between the loss-of-function *SCN5A* mutation and arrhythmogenesis in BrS patients remains unclear.

The interaction between cellular abnormalities and tissue properties changes is essential for comprehensively understanding the arrhythmic mechanism of BrS. The first assignment developed and fitted a Markov model to simulate the AP duration (APD) and morphology in both wild-type (WT) and *SCN5A* mutation (MT). As a result, we observed the same APD between WT and MT, but the difference was the loss of AP dome in the epicardium which is the key feature of BrS. The second assignment identified that heart areas representing steep repolarization time gradient (RTG) caused by scars were vulnerable to arrhythmias**.** Indeed, at tissue level, fibrosis and RTG arise by local differences in AP can exacerbate conduction heterogeneity, thus providing a substrate for re-entry (5, 6). Therefore, this assignment aims to elucidate the mechanisms of how loss of AP dome caused by Na+ channel mutation forms RTG, how RTG and fibrosis cause unidirectional block and create substrates for re-entry, and finally how re-entry induces arrhythmias in BrS patients.

Methods

To simulate the effect of *SCN5A* mutation on cellular and tissue levels of AP in OpenCARP, TenTusscher model (TT2) (7) was selected for these reasons: (1) a realistic simulation approach for both human ventricular myocytes and tissue, (2) easily modifying parameters to mimic AP properties associated with BrS, and (3) being successfully used to model BrS and arrhythmias in previous studies (8-11). The TT2 model was initially adapted in OpenCARP (01_EP_single cell/ 01_basic_bench) to simulate a single cell's APD in WT and MTs when the maximum Na+ conductance (GNa) was reduced by 75%, 50%, and 25% respectively to mimic the effects in BrS. As mutations increasing Ito activity and diminishing ICaL activity are also observed in BrS, the maximum conductance of epicardial Ito (Gto) was increased by 200% while the maximum conductance of epicardial ICaL (GCaL) was reduced by 100% to simulate the severity of the disease. Next, the effects of BrS at 2D tissue level were investigated using the same TT2 model in OpenCARP (02_EP_tissue/08_lats) by reducing GNa to 75%, 50%, and 25% of intensity. 2D maps of the local activation time (LAT) and APD at different mutant conditions were then generated to explore the formation of RTG.

Mitchell Schaeffer model in the EPSimulator website (https://epsimulator.grantorai.com/) was used to investigate the re-entrant arrhythmia mechanism. This is a simple model with only two variables: an inward current combining Na^+ and Ca^{2+} channels and an outward current of the K^+ channel to replicate the behavior of ventricular AP (12). This model can also simulate wave propagation in 2D tissue and arrhythmias by adjusting RTG and fibrosis area. In tissue setting, RTG was modified with different ranges, including 40 – 120 *ms* and 60 – 100 *ms*, to examine the influence of RTP steepness on arrhythmia risk. Similarly, different fibrosis radii from 5 to 15 and 30 were analyzed to identify how changes in fibrosis area increase the risk of arrhythmias. Finally, appropriate S1-S2 protocols were applied in each condition by adjusting the start time of the S2 stimulus to identify the coupling interval (CI) whose lowest value and highest value triggering arrhythmia were considered the lower bound and higher bound of the vulnerable window, respectively.

Results

Lower GNa did not change the APD but resulted in a smaller peak current during the upstroke of AP, causing a loss of AP dome which was also found in mini-assignment 1 (**Figure 1**). A gain-of-function mutation in Ito by increasing Gto to 300% showed a deep notch in epicardial AP, whereas, a loss-of-function mutation in ICaL by fully blocking it caused a shorter epicardial AP (**Figure 2A-B**). When these mutations were combined into the TT2 model, the interchange of short triangular APs and deep notch-shaped APs was seen in the epicardium (**Figure 2C**). All of these findings are typical for BrS.

In the 2D tissue model, reduced GNa significantly increased the LAT, particularly, LATs ranged from 2.1 - 20.3 *ms* in WT, 2.3 - 22.3 *ms* in 75% of GNa, 2.4 - 25.9 *ms* in 50% of GNa, and 9.8 - 36.2 *ms* in 25% of GNa (**Figure 3**). APD maps showed consistency with cellular APD since the duration did not change significantly. APDs ranged from 259.5 – 267.7 *ms* in WT, 259.8 – 268.8 *ms* in 75% of GNa, 259.6 – 268.2 *ms* in 50% of GNa, and 258.4 – 267.6 *ms* in 25% of GNa (**Figure 4**). Although mutation in Na+ channel could not significantly alter APD, the resulting gradient of LAT was still able to create a gradient of repolarization time since the activation time is equal to APD plus repolarization time.

Both RTG and fibrosis could induce arrhythmia at the appropriate S1-S2 protocol. The vulnerable window of arrhythmia regarding RTG from 60 – 100 *ms* was between 440 – 455 *ms*. When RTG was expanded to 40 – 120 *ms*, the vulnerable window was from 455 *ms* to 475 *ms* (**Figure 5**). These findings suggested that steeper RTG may increase the risk of re-entrant arrhythmia by increasing the range of vulnerable window. Moreover, the vulnerable window inducing arrhythmia was 420 – 440 *ms* in the heart with fibrosis radius of 5, was 425 – 440 ms with fibrosis radius of 15, and was 430 – 445 *ms* with fibrosis radius of 30 (**Figure 6**). **Figure 7** shows the combined effect of RTG (40 – 100 *ms*) and fibrosis (radius = 20) on arrhythmogenesis at CI = 425 *ms*, indicating that both RTG and fibrosis would serve as substrates for re-entry while premature S2 beat triggered it to initiate arrhythmias.

Discussion

In this study, TT2 model showed a loss of AP dome caused by Na^+ mutation, but a little change in APD. Properties of BrS were also observed in epicardium with increased Ito or decreased ICaL, suggesting alternative candidates for BrS when no mutations in *SCN5A* are detected. The Mitchell Schaeffer model revealed that RTG created by mutation and fibrosis led to unidirectional block and offered a potential substrate for re-entry while premature beat triggered it. Both re-entry circuit and fibrosis are underlying mechanisms of arrhythmia. These findings are in good accordance with results from mini-assignments 1 and 2, demonstrating this study's capability in properly simulating re-entrant arrhythmia in Brugada patients.

Reduced INa which affects depolarization is not able to counteract the Ito current, especially in the right ventricular epicardium where Ito is stronger, thus leading to early repolarization and loss of AP dome but the same APD (4). Loss of AP dome further results in ST-segment elevation and T-wave inversion on the ECG which are typical for BrS. Moreover, loss of AP dome in the epicardium is usually heterogeneous, thus creating the dispersion of repolarization and refractoriness which are responsible for developing a vulnerable window where premature beat can trigger re-entry (13). When a premature beat occurs, it can propagate in the direction where tissue has recovered but is blocked in the direction where tissue is still refractory, resulting in the unidirectional block which initiates arrhythmia (14). The second mechanism is phase 2 re-entry which happens when the conduction propagating from dome-preserved sites to dome-lost sites can locally re-excite epicardium with premature repolarization, thus triggering arrhythmias (13). In both mechanisms, steeper RTG characterized by larger dispersity over a shorter distance is more likely to increase the risk of arrhythmogenesis (14).

In the fibrosis area, non-excitable cardiac fibroblasts abnormally proliferate and secrete collagen fibers, leading to the structural heterogeneity of myocardial tissue (6, 15). This tissue remodeling changes ionic channels properties, cell size, and then overall heart structure, thereby slowing conduction and causing unidirectional block (6). These functional and structural blocks create substrates for arrhythmia and thus being considered arrhythmogenic conditions (16). Although it has been believed that larger area of fibrosis increases the risk of arrhythmias by expanding vulnerable window (17), this study did not observe this finding for different fibrosis radii, possibly due to Mitchell Schaeffer model's simplicity and AI-based EPSimulator's low reliability. As this model ignores detailed interactions between inward and outward currents, it is unable to capture exactly small changes in recovery time, which is important to identify appropriate start time of premature beats. Plus, this model lacks experimental validation and confident intervals for predictions, thus reducing its reliability in clinical application (18). Therefore, future improvements and validations increasing the complexity and reliability are crucial for this model to accurately capture the changes in APD and electrical propagation.

Although TT2 model is a powerful approach for simulating APD in BrS and arrhythmias, it still remains several limitations, such as absence of Na^+, K^+, and intracellular Ca^{2+} dynamics, or steady-state assumptions for the fast activating gates of Ito, IKr, and ICaL which cause instantaneous activation instead of time-delaying (8). These drawbacks influence the accuracy and applicability of modeling results. Therefore, future studies are required to refine this model or develop alternative models that can precisely and efficiently simulate changes in AP duration and morphology across different mutation types.

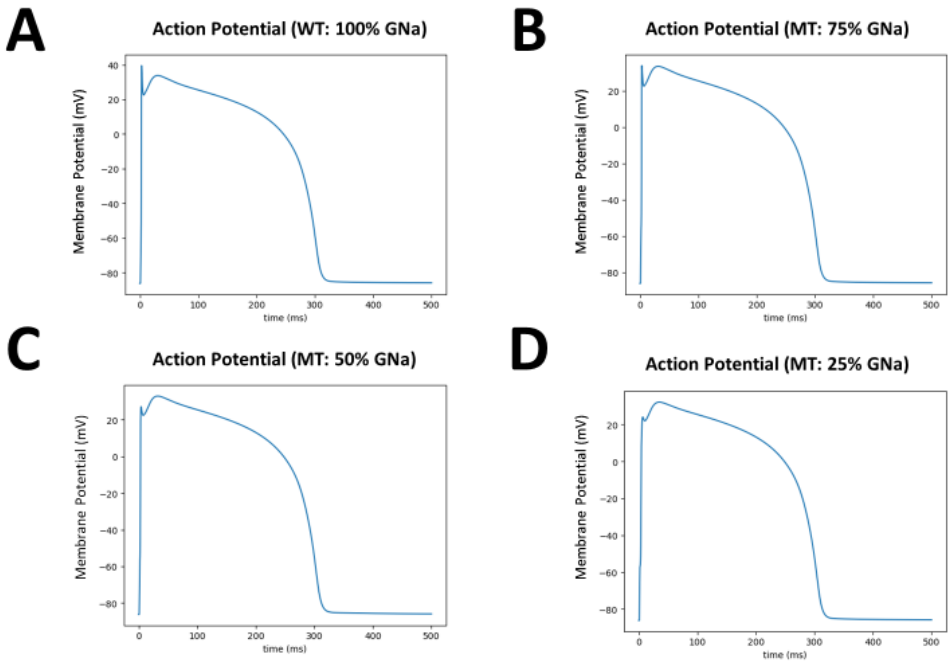

Figure 1: Steady-state action potentials (BCL = 1000 *ms*) of epicardial cells in the TT2 model for the default setting of WT (**A**), for modified 75% of INa current (**B**), for 50% of INa current (**C**), and for 25% of INa current (**D**). BCL: basic cycle length.

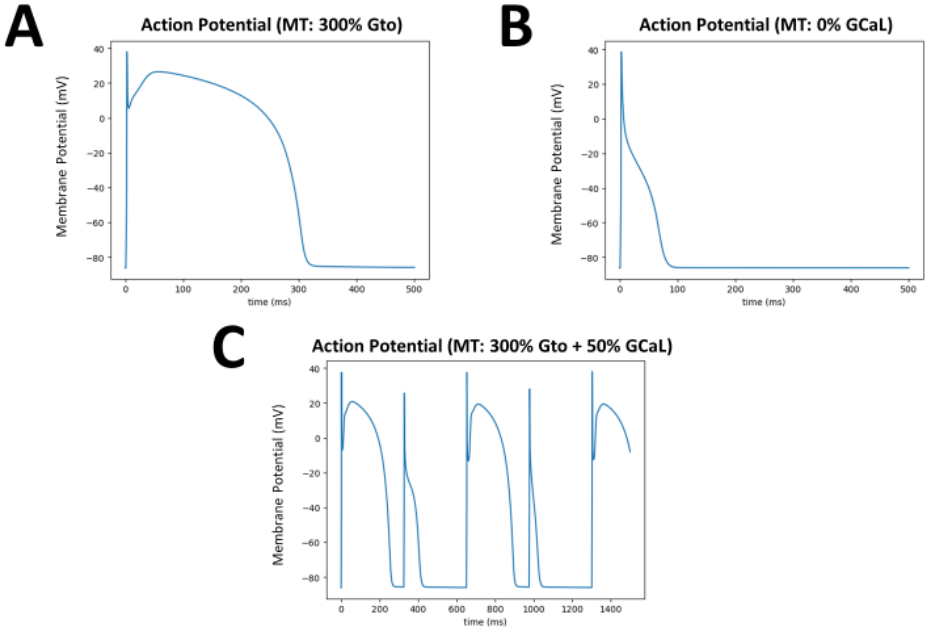

Figure 2: Epicardium with a deep notch and the Brugada syndrome in the TT2 model. (**A**) Epicardial action potential with a deep notch (BCL = 1000 *ms*) resulted from an Ito gain-of-function mutation. (**B**) Epicardium with a short triangular shape of action potential (BCL = 1000 *ms*) resulted from an ICaL loss-of-function mutation. (**C**) Brugada syndrome: the interchange of short triangular and deep notch-shaped action potentials in the epicardium (BCL = 325 *ms*) as a result of combined Ito mutation and ICaL mutation. BCL: basic cycle length.

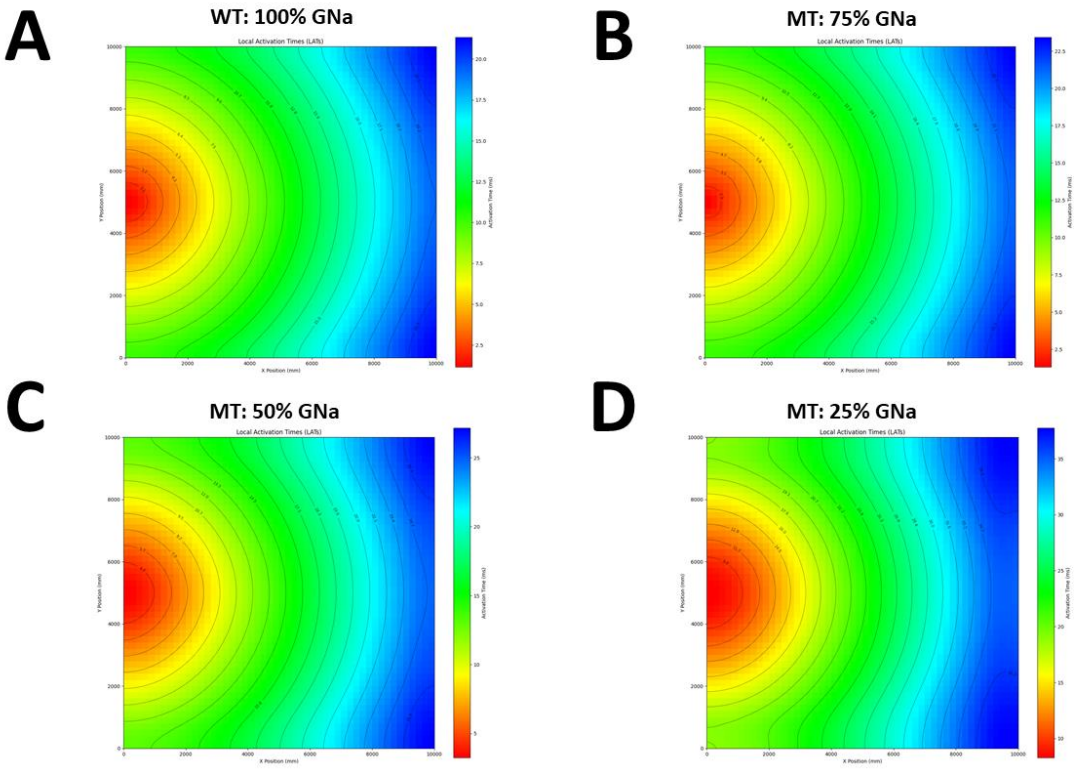

Figure 3: 2D maps of local action times at 2D tissue level in the TT2 model for the default setting of WT (**A**), for modified 75% of INa current (**B**), for 50% of INa current (**C**), and for 25% of INa current (**D**).

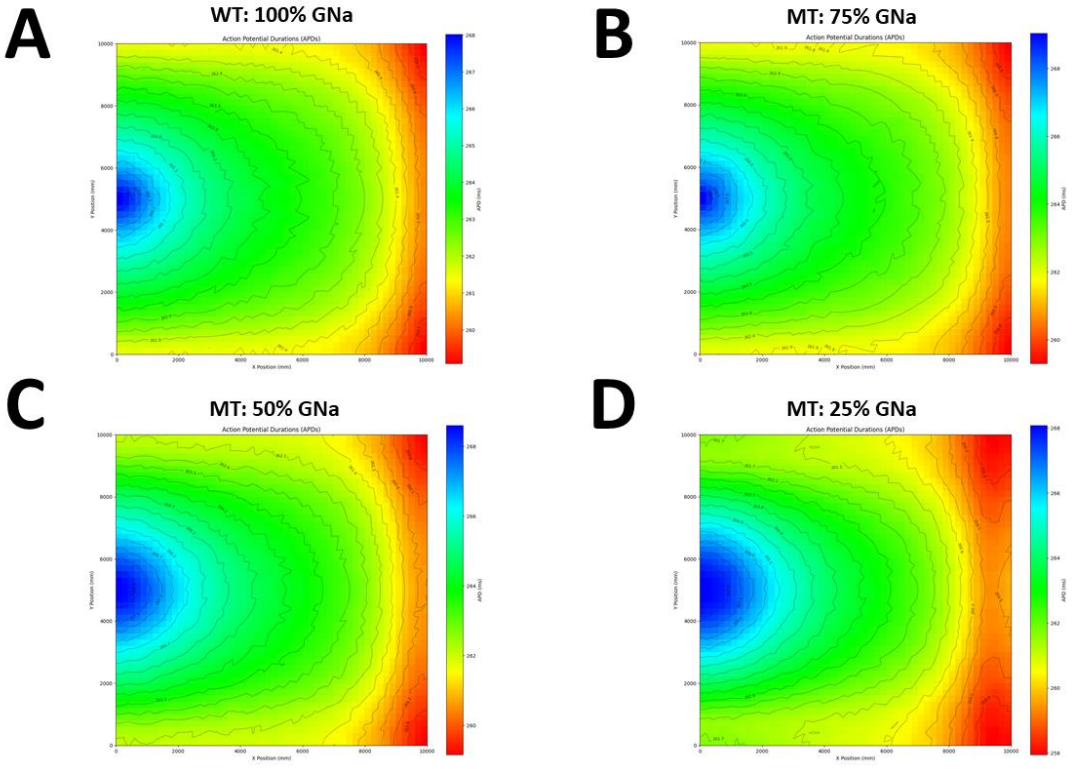

Figure 4: 2D maps of action potential duration at 2D tissue level in the TT2 model for the default setting of WT (**A**), for modified 75% of INa current (**B**), for 50% of INa current (**C**), and for 25% of INa current (**D**).

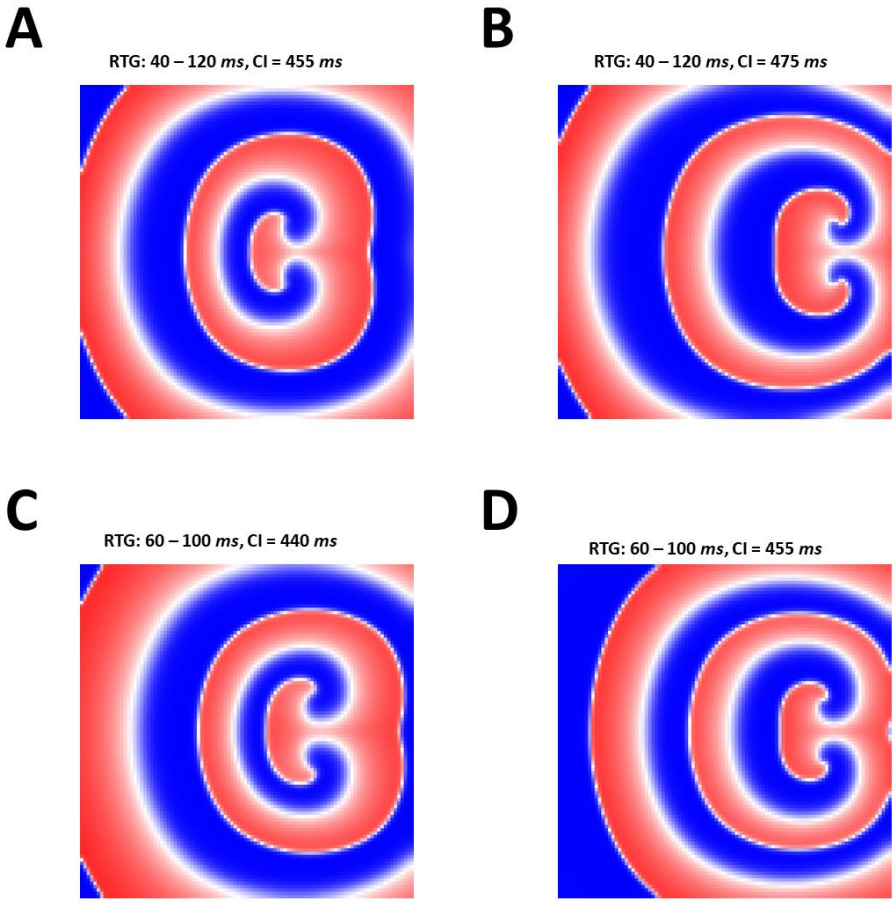

Figure 5: Re-entry-based arrhythmic behavior and vulnerable windows at different steepness of RTG in EPSimulator. (**A**) Arrhythmia observed at lower bound (CI = 455 *ms*, simulating time = 1238) of vulnerable window with RTG ranging from 40 *ms* to 120 *ms*. (**B**) Arrhythmia observed at upper bound (CI = 475 *ms*, simulating time = 1270) of vulnerable window with of RTG ranging from 40 *ms* to 120 *ms*. (**C**) Arrhythmia observed at lower bound (CI = 440 *ms*, simulating time = 1208) of vulnerable window with RTG ranging from 60 *ms* to 100 *ms*. (**D**) Arrhythmia observed at upper bound (CI = 455 *ms*, simulating time = 1184) of vulnerable window with RTG ranging from 60 *ms* to 100 *ms*. Tissue settings: diffusion coefficient = 0.1, rows = 100, columns =100, parameter tau_in = 0.3, parameter tau_out = 6, parameter tau_open = 120, parameter tau_close = 80, S1-S2 protocol: S1 stimulus start time = 1 *ms*, S1 stimulus duration = 1 *ms*, S2 stimulus start time = 455/475/440 *ms* depending on simulated conditions, S2 stimulus duration = 1 *ms*, simulation duration = 1500, repolarization gradient: left value = 40/60 *ms*, right value = 120/100 *ms* depending on simulated conditions. RTG: repolarization time gradient, CI: coupling interval.

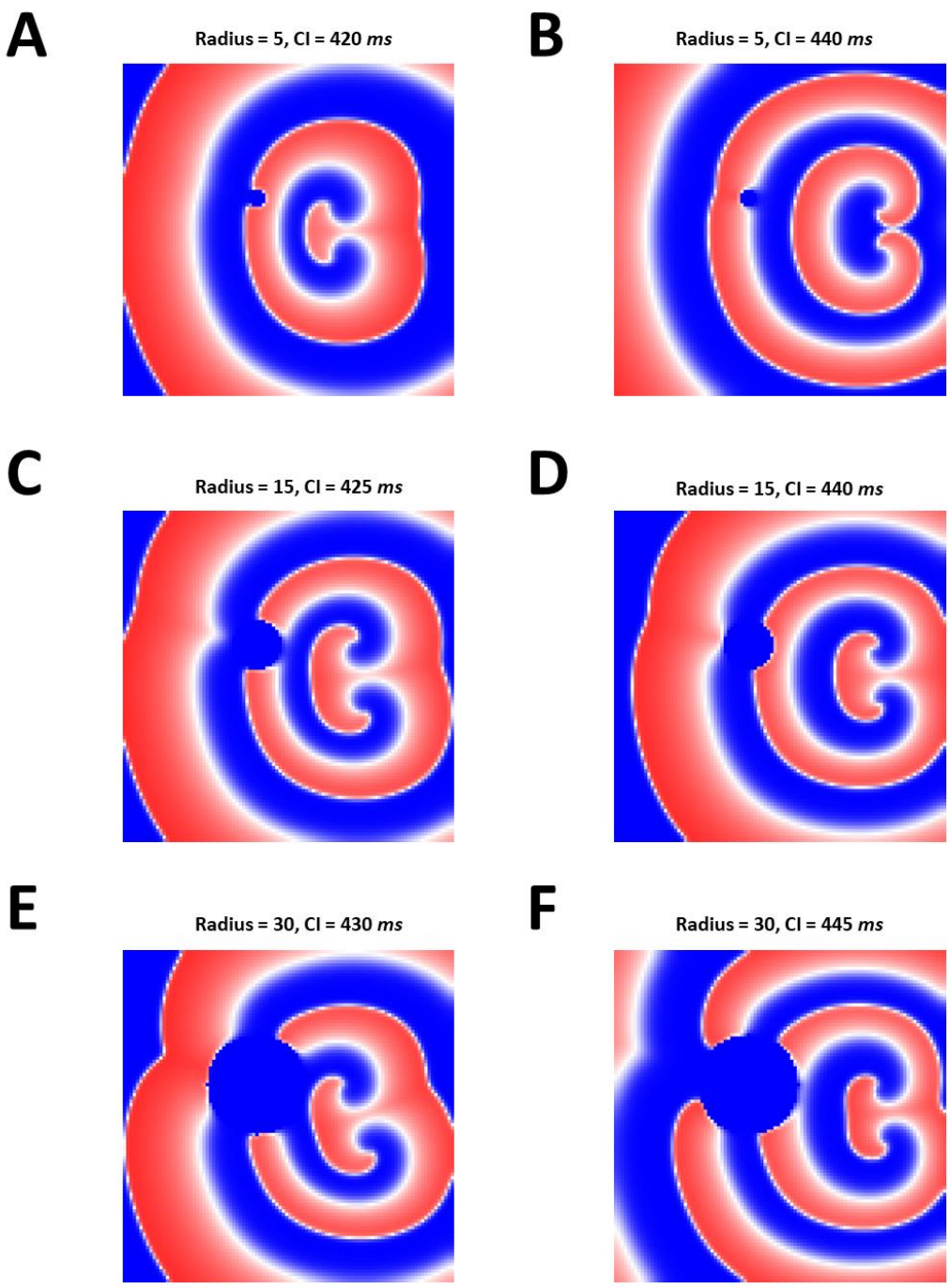

Figure 6: Re-entry-based arrhythmic behavior and vulnerable windows at different fibrosis radii in EPSimulator. (**A**) Arrhythmia observed at lower bound (CI = 420 *ms*, simulating time = 998) of vulnerable window with fibrosis radius = 5. (**B**) Arrhythmia observed at upper bound (CI = 440 *ms*, simulating time = 1070) of vulnerable window with fibrosis radius = 5. (**C**) Arrhythmia observed at lower bound (CI = 425 *ms*, simulating time = 1000) of vulnerable window with fibrosis radius = 15. (**D**) Arrhythmia observed at upper bound (CI = 440 *ms*, simulating time = 980) of vulnerable window with fibrosis radius = 15. (**E**) Arrhythmia observed at lower bound (CI = 430 *ms*, simulating time = 1000) of vulnerable window with fibrosis radius = 30. (**F**)Arrhythmia observed at upper bound (CI = 445 *ms*, simulating time = 1142) of vulnerable window with fibrosis radius = 30. Tissue settings: diffusion coefficient = 0.1, rows = 100, columns =100, parameter tau_in = 0.3, parameter tau_out = 6, parameter tau_open = 120, parameter tau_close = 80, S1-S2 protocol: S1 stimulus start time = 1 *ms*, S1 stimulus duration = 1 *ms*, S2 stimulus start time = 420/425/430/440/445 *ms* depending on simulated conditions, S2 stimulus duration = 1 *ms*, simulation duration = 1500, obstacle radius = 5/15/30 depending on simulated conditions. CI: coupling interval.

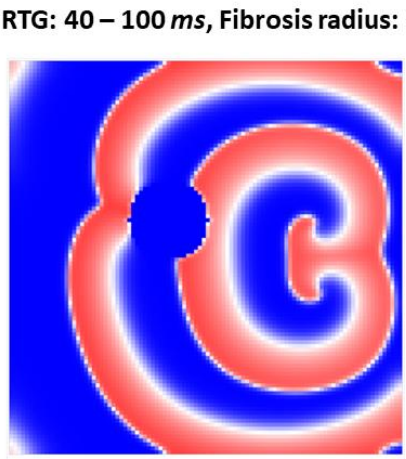

Figure 7: Combined effects of RTG (40 – 100 *ms*) and fibrosis (radius = 20) on initiating re-entrant arrhythmia (CI = 425 *ms*). Tissue settings: diffusion coefficient = 0.1, rows = 100, columns =100, parameter tau_in = 0.3, parameter tau_out = 6, parameter tau_open = 120, parameter tau_close = 80, S1-S2 protocol: S1 stimulus start time = 1 *ms*, S1 stimulus duration = 1 *ms*, S2 stimulus start time = 425 *ms*, S2 stimulus duration = 1 *ms*, simulation duration = 1500, repolarization gradient: left value = 40 *ms*, right value = 100 *ms*, obstacle radius = 20. RTG: repolarization time gradient, CI: coupling interval.

References

1. El Sayed M, Goyal A, Callahan AL. Brugada syndrome. StatPearls [Internet]: StatPearls Publishing; 2023.
2. Malik BR, Rudwan AMA, Abdelghani MS, Mohsen M, Khan SHA, Aljefairi N, et al. Brugada syndrome: clinical features, risk stratification, and management. Heart Views. 2020;21(2):88-96.
3. van Hoorn F, Campian ME, Spijkerboer A, Blom MT, Planken RN, van Rossum AC, et al. SCN5A mutations in Brugada syndrome are associated with increased cardiac dimensions and reduced contractility. 2012.
4. Tsumoto K, Ashihara T, Naito N, Shimamoto T, Amano A, Kurata Y, et al. Specific decreasing of Na+ channel expression on the lateral membrane of cardiomyocytes causes fatal arrhythmias in Brugada syndrome. Scientific reports. 2020;10(1):19964.
5. Meo M, Bonizzi P, Bear LR, Cluitmans M, Abell E, Haïssaguerre M, et al. Body surface mapping of ventricular repolarization heterogeneity: an ex-vivo multiparameter study. Frontiers in physiology. 2020;11:933.
6. Kazbanov IV, Ten Tusscher KH, Panfilov AV. Effects of heterogeneous diffuse fibrosis on arrhythmia dynamics and mechanism. Scientific reports. 2016;6(1):20835.
7. Repository CM. ten Tusscher, Panfilov, 2006 [Available from: https://models.cellml.org/exposure/de5058f16f829f91a1e4e5990a10ed71.
8. Ten Tusscher KH, Panfilov AV. Cell model for efficient simulation of wave propagation in human ventricular tissue under normal and pathological conditions. Physics in Medicine & Biology. 2006;51(23):6141.
9. Xia L, Zhang Y, Zhang H, Wei Q, Liu F, Crozier S. Simulation of Brugada syndrome using cellular and three-dimensional whole-heart modeling approaches. Physiological Measurement. 2006;27(11):1125.
10. Ten Tusscher KH, Noble D, Noble P-J, Panfilov AV. A model for human ventricular tissue. American Journal of Physiology-Heart and Circulatory Physiology. 2004;286(4):H1573-H89.
11. Ten Tusscher KH, Bernus O, Panfilov AV. Comparison of electrophysiological models for human ventricular cells and tissues. Progress in biophysics and molecular biology. 2006;90(1-3):326-45.
12. Repository CM. Mitchell, Schaeffer, 2003 [Available from: https://models.cellml.org/exposure/4b4acf2c64cecd7203c9b748cc4508a5.
13. Antzelevitch C. Late potentials and the Brugada syndrome. American College of Cardiology Foundation Washington, DC; 2002. p. 1996-9.
14. Rudy Y. Noninvasive mapping of repolarization with electrocardiographic imaging. 2021. p. e021396.
15. Platonov PG. Atrial fibrosis: an obligatory component of arrhythmia mechanisms in atrial fibrillation? Journal of geriatric cardiology: JGC. 2017;14(3):174.
16. De Jong S, van Veen TA, van Rijen HV, de Bakker JM. Fibrosis and cardiac arrhythmias. Journal of cardiovascular pharmacology. 2011;57(6):630-8.

17. de Jong S, van Veen TA, de Bakker JM, Vos MA, van Rijen HV. Biomarkers of myocardial fibrosis. Journal of cardiovascular pharmacology. 2011;57(5):522-35.
18. Gillette K, Gsell MA, Strocchi M, Grandits T, Neic A, Manninger M, et al. A personalized real-time virtual model of whole heart electrophysiology. Frontiers in Physiology. 2022;13:907190.